Spin-tensor analysis of realistic shell model interactions

E. Osnes
Department of Physics, University of Oslo, Blindern, Oslo 3, Norway

D. Strottman
Theoretical Division, Los Alamos National Laboratory, Los Alamos, New Mexico 87545
(Received 16 September 1991)

In this paper various realistic shell model effective interactions are analyzed in terms of their central, vector, and tensor components. The effective forces were obtained from phenomenological (Hamada-Johnston) as well as from modern meson-exchange (Bonn-Jülich and Paris) nucleon-nucleon potentials and were calculated to various approximations within the framework of perturbation theory. For all forces examined, the dominant contribution comes from the central part. The vector component is small for the bare G-matrix interaction, especially for $T = 0$, but is considerably modified by renormalization. The tensor component is somewhat larger than the vector component and is relatively larger for the Hamada-Johnston potential than for the Bonn-Jülich and Paris potentials. Centroids in j-j and SU(3) coupling were obtained with and without noncentral contributions; considerable sensitivity was observed in the SU(3) basis.

PACS number(s): 21.60.Fw, 21.60.Cs, 21.30.+y

I. INTRODUCTION

In this paper we examine various realistic shell model effective interactions in terms of their central, vector, and tensor components and their transformation properties under SU(3) and SU(4). These components can be separated out by performing a spin-tensor decomposition of the interaction. Such a decomposition may be helpful in revealing the physical properties of the effective interaction, which is a complex entity. In fact, the evaluation of the shell model effective interaction from the underlying free nucleon-nucleon (NN) interaction is one of the outstanding problems of nuclear many-body theory. This is an exceedingly complicated problem which, despite much progress made over the last 25 years, cannot be considered settled. Thus, efforts are continuously being made to solve this problem as well as to determine the essential details of the interaction that determine the structure of systems of several nucleons.

There are several obstacles to the accomplishment of this program. The first problem is associated with the choice of the NN interaction. This can be either of phenomenological nature [1, 2], obtained by fitting phase shifts of NN scattering and the deuteron properties, or of more fundamental nature, calculated by meson-exchange theory [3, 4]. In principle, the NN interaction should be calculable from the underlying quark-gluon interaction, but such calculations have not been able to reproduce realistic NN interactions. Roughly speaking, typical phenomenological NN interactions, such as the Hamada-Johnston [1] and Reid potentials [2], differ from the more modern Paris [3] and Bonn-Jülich [4] meson-exchange potentials in the strength of the much debated tensor-force component. The former have rather strong tensor components whereas the latter have somewhat weaker tensor components. In meson-exchange models the tensor component results from a partial cancellation of the tensor components from π- and ρ-meson exchanges. The larger the ρN coupling constant, the better the cancellation. Although the phenomenological potentials are not explicitly constructed in terms of meson exchanges, the effective ρN coupling is much weaker in these, corresponding to a stronger tensor component [5]. Although a finite tensor component is needed in the effective interaction to reproduce observed nuclear properties (e.g., the β decay in the mass 14 system), it seems desirable for the convergence properties of the effective interaction evaluated by many-body perturbation theory that the tensor component be fairly weak. However, more work is needed before this question can be definitely answered.

The second problem in obtaining the effective interaction is associated with its evaluation by many-body perturbation methods, once the initial NN interaction has been chosen. This procedure generally includes two steps. First, since the NN interaction is strongly singular at short internucleon distances, it has to be regularized in some way before it can be used in a perturbative treatment. This is generally achieved by evaluating the Bethe-Brueckner-Goldstone reaction matrix G which incorporates the two-nucleon short-range correlations by allowing the two nucleons to interact virtually any number of times as shown in Fig. 1(a). Then, in the second step one uses the reaction matrix G as a starting point for a perturbation expansion of the effective interaction. The philosophy regarding which diagrams to include differs widely. For example, one could either sum the diagrams order by order in G or carry out infinite summations of subsets of diagrams. In both cases, of course, one has to be rather selective in choosing the diagrams to be included. Thus, in practice there is no definite procedure for obtaining the effective interaction once the NN interaction has been chosen and the G matrix evaluated.

Furthermore, any procedure for obtaining the effective interaction from a given NN interaction is rather intricate. Thus, in the end it may be difficult to tell precisely which features of the original NN interaction are important for the resulting effective interaction, and all the more so as the effective interaction is not obtained in analytic form but in terms of its matrix elements. The effective interactions obtained by the various approximations will therefore have to be assessed from their merits, i.e., from their ability to describe nuclear properties, such as spectra, decay rates, and reaction cross sections.

To date, several reasonable effective interactions have been obtained. In order to understand their differences on a more fundamental level than just comparing energy spectra and related properties, it may be instructive to analyze the various interactions in terms of their spin-tensor components. In particular, it is of interest to see to what extent the presumed different tensor strengths in the original NN interactions show up in the corresponding G matrices and renormalized effective interactions. Another reason for carrying out a spin-tensor decomposition of the effective interaction is to get an assessment of the salient features which have to be incorporated into effective interactions for heavier nuclei which are not easily calculable from many-body theory because of the many single-particle degrees of freedom involved.

A few spin-tensor analyses have actually been carried out for ($1s0d$) shell effective interactions [6–10], for both calculated and empirical ones. For the present work we wish to compare several calculated effective interactions which have all proven rather successful in reproducing nuclear properties. These interactions will be discussed in Sec. II. In Sec. III we recall briefly the basic steps involved in carrying out a spin-tensor decomposition. The results are presented and discussed in Sec. IV, and we summarize our findings in Sec. V.

II. EFFECTIVE INTERACTIONS

In this section we shall briefly discuss the effective interactions which are to be analyzed in terms of their spin-tensor components. We consider two classes of interactions. One class [11, 12] is derived from the phenomenological Hamada-Johnston potential which has a rather strong tensor component, while the other class [13–15] is derived from meson-exchange potentials such as the Paris or Bonn-Jülich potentials which have somewhat weaker tensor components. Within each class of interaction we consider the effect of various renormalizations. We also examine the effect of expressing the effective interaction in a Hartree-Fock (HF) single-particle basis rather than in the conventional harmonic-oscillator basis. The various approximations are listed in Table I.

As an example of an effective interaction derived from the phenomenological Hamada-Johnston NN potential, as well as a standard of reference, we consider the interaction derived in the pioneering works of Kuo and Brown [11]. As is well known and shown in Fig. 2, the bare G matrix [Fig. 1(a)] evaluated by Kuo and Brown is not sufficient to describe the energy spectrum of two nucleons outside a closed shell. In fact, an insufficient ground-state binding energy is obtained and the spectrum is too compressed. In order to increase the binding energy and expand the spectrum, it is necessary to

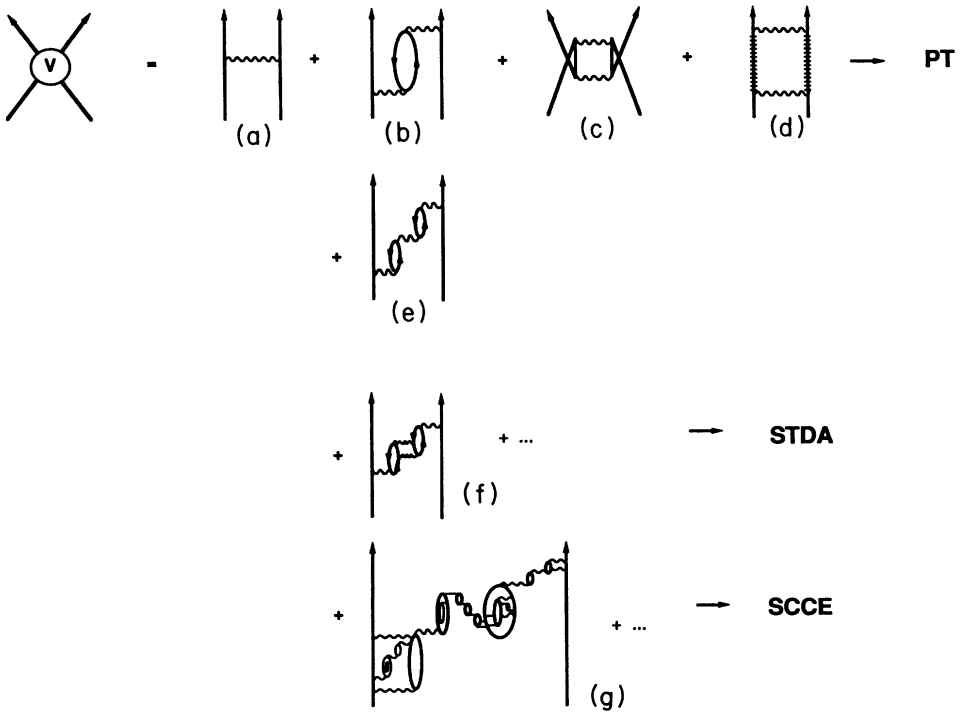

FIG. 1. Approximations considered for the effective interaction. Shown are the diagrams contributing to the approximations G, PT, STDA, and SCCE listed in Table I.

TABLE I. Effective interactions analyzed by spin-tensor decomposition. The various approximations considered are defined in terms of their diagrammatic expansions in Fig. 1. Note that respectively approximations PT and STDA for the Hamada-Johnston, and approximations SCCE and $(SCCE)_{HF}$ for the Bonn-Jülich and Paris potentials, are not directly comparable since they include different approximations to the interaction.

Phenomenological	Meson exchange	
Hamada-Johnston	Bonn-Jülich	Paris
G[a]	G[c]	G[e]
PT[a]	SCCE[d]	SCCE[d]
STDA[b]	$(SCCE)_{HF}$[d]	$(SCCE)_{HF}$[d]

[a] Reference [11].
[b] Reference [12].
[c] Reference [14].
[d] Reference [15].
[e] References [8, 13].

include second-order corrections in G through perturbation theory. These corrections are the three-particle, one-hole or core-polarization contribution, Fig. 1(b), the four-particle, two-hole contribution, Fig. 1(c), and the two-particle contribution, Fig. 1(d). The resulting interaction is denoted by PT. In particular, the second-order core-polarization term shown in Fig. 1(b) produces the desired effect. As an extension we consider the interaction derived by Kuo and Osnes [12] by summing the infinite set of core-polarization diagrams [Figs. 1(b), 1(e), ...], using particle-hole vertices screened to second order as shown in Fig. 1(f). This approximation may be called the screened Tamm-Dancoff approximation (STDA) and is shown in Fig. 2 to produce results similar to second-order perturbation theory (PT).

In the class of meson-exchange potentials we consider the Paris and Bonn-Jülich potentials. For these potentials we compare the bare G-matrix interaction [13, 14] with a renormalized interaction [15] containing essentially all important long-range correlations to arbitrary order as shown in Fig. 1(g). As the evaluation of this interaction involves solving a self-consistent set of coupled equations, it is denoted by SCCE. In fact, it was found that this interaction was too strongly attractive for the low-spin states, as shown in Fig. 2. A more reasonable interaction could be obtained, however, by employing a HF basis for the single-particle states, provided that the collective four-particle, two-hole (4p-2h) correlations, which cannot easily be incorporated by perturbation theory, be explicitly included.

In Fig. 2 we have only shown the T=1 spectra for two nucleons outside an ^{16}O closed core. However, qualitatively similar results are obtained for the T=0 spectra. The Paris potential gives results similar to the Bonn-Jülich potential for the bare T=1 G-matrix interaction. The T=0 Paris bare G matrix is, however, considerably less attractive than the Bonn-Jülich G matrix. Clearly, this results in less bound states for both T=0 and T=1 in all the higher-order approximations for the Paris potential, as shown in detail in Ref. [15]. Also shown in

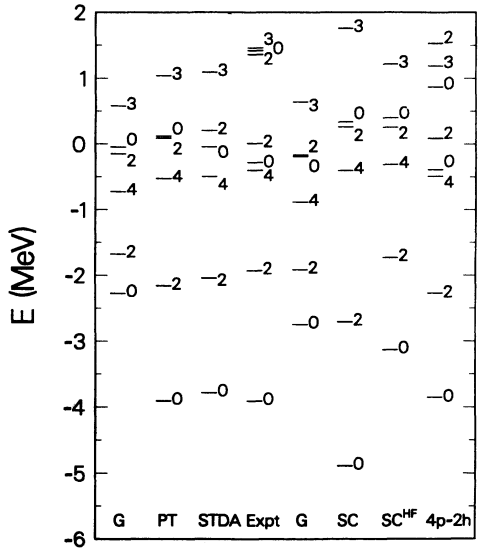

FIG. 2. Low-energy spectrum of ^{18}O calculated for the various approximations of the effective interaction defined in Fig. 1 and Table I. In the figure caption SCCE is abbreviated as SC and 4p-2h refers to results including intruder states, Ref. [16].

the far right column are results obtained by explicitly including low-lying, deformed four-particle, two-hole states [16]. The required additional matrix elements were taken from the phenomenological weak-coupling calculations of Ellis and Engeland [16]. The inclusion of these so-called intruder states are seen to restore the spectrum in near agreement with experiment.

III. SPIN-TENSOR DECOMPOSITION

The calculational procedure for a spin-tensor analysis is well known. It rests on the fact that any scalar two-particle interaction V can be expanded in terms of spherical tensors as

$$V = \sum_k \mathbf{Q}^{(k)} \cdot \mathbf{S}^{(k)} = \sum_{k,\kappa} (-)^{\kappa} Q_{\kappa}^{(k)} S_{-\kappa}^{(k)} \equiv \sum_k \mathcal{V}_k, \qquad (1)$$

where $Q_{\kappa}^{(k)}$ and $S_{\kappa}^{(k)}$ are spherical tensors of rank k and component κ in configuration and spin spaces, respectively. The summation runs over k = 0, 1, and 2. The corresponding components $\mathcal{V}_k$ of the interaction are called the central, vector, and tensor components. The vector component is also called the two-body spin-orbit term. (In addition to the ordinary two-body spin-orbit term, the vector term also contains the so-called antisymmetric spin-orbit term [17]; we will, however, not be concerned with this distinction here.) By standard angular momentum algebra it is straightforward to evaluate the matrix elements of $\mathcal{V}_k$ from the matrix elements of V.

The first step in the decomposition is to transform the jj-coupled matrix element of $\mathcal{V}_k$ to LS coupling

$$< \alpha\beta JT|\mathcal{V}_k|\gamma\delta\, JT >= \sum_{LL'SS'} U \begin{pmatrix} \ell_a \frac{1}{2} j_a \\ \ell_b \frac{1}{2} j_b \\ L\ S\ J \end{pmatrix} U \begin{pmatrix} \ell_c \frac{1}{2} j_c \\ \ell_d \frac{1}{2} j_d \\ L'\ S'\ J \end{pmatrix} < abLSJ|\mathcal{V}_k|cd\, L'S'J >, \tag{2}$$

where $\alpha \equiv (n_a, \ell_a, j_a)$ and $a \equiv (n_a, \ell_a)$, etc. Note that in our notation the coefficient $U(\cdots)$ is a unitary 9-j symbol, related to the usual 9-j symbol by

$$U \begin{pmatrix} a\ b\ c \\ d\ e\ f \\ g\ h\ i \end{pmatrix} = \sqrt{(2c+1)(2f+1)(2g+1)(2h+1)} \begin{Bmatrix} a\ b\ c \\ d\ e\ f \\ g\ h\ i \end{Bmatrix}.$$

Thus, the LS-coupled matrix element of $\mathcal{V}_k$ on the right-hand side of Eq. (2) can be expressed in terms of matrix elements of the total V by replacing $\mathcal{V}_k = \mathbf{Q}^{(k)} \cdot \mathbf{S}^{(k)}$ from Eq. (1), using the Wigner-Eckart theorem and inverting the relation using the orthogonality properties of the 6j symbols:

$$< abLSJ|\mathcal{V}_k|cd\, L'S'J >= (2k+1) \begin{Bmatrix} L\ S\ J \\ S'\ L'\ k \end{Bmatrix} \sum_{J'} (-)^{J'} (2J'+1) \begin{Bmatrix} L\ S\ J' \\ S'\ L'\ k \end{Bmatrix} < abLSJ'|\mathcal{V}|cd\, L'S'J' > . \tag{3}$$

The two-particle matrix elements are normalized and antisymmetrized.

The LS-coupling matrix elements in Eq. (3) are obtained from the jj-coupling matrix elements by the usual expression which is the inverse of Eq. (2). In the beginning of the (1s0d) shell the SU(3)⊂SU(6) scheme provides a much more viable coupling scheme than does jj coupling as well as providing for physical insight into the structure calculations. For the two-particle system, the allowed SU(6) representations are the spatially symmetric [**2**] and the antisymmetric [**11**] states. The corresponding SU(3) representations are (4 0) and (0 2) for the symmetric states and (2 1) for the antisymmetric state. In this scheme the centroids have a particularly appealing property: only the central (k=0) components contribute; the contributions from the k=1 and k=2 components sum to zero. In addition, previous work [8] has shown that even in cases where there are no discernable differences in centroids calculated in jj coupling, large differences may appear in SU(3) coupling. The transformation from LS coupling to SU(3) is implemented by the use of the appropriate SU(3) vector coupling coefficients which we take from Draayer and Akiyama [18].

Finally, in analogy with Eq. (3) above, the two-body interaction V may be expressed [20] in terms of SU(3) tensors $(\lambda_k \mu_k)$ by multiplying the SU(3) coupled two-body matrix elements by the Wigner coefficient $(-)^{\lambda+\mu} < (\lambda\mu)KL\ \overline{(\mu'\lambda')}K'L'|(\lambda_k\mu_k)K_kL_k >$ and summing over the relevant quantum numbers. The relevant SU(3) operators $(\lambda_k \mu_k)$ for our discussion are those contained in (40) × (04) or (04) × (20) and which admit rank-zero interactions, namely, (0 0), (2 2), (2 4) + (4 2), and (4 4). In a similar fashion the tensor operators may be coupled to specific SU(4) representations.

IV. DISCUSSION OF RESULTS

A. Hamada-Johnston potential

In Fig. 3 we show the contributions from the various spin-tensor components of the diagonal $T = 1$ and $T = 0$

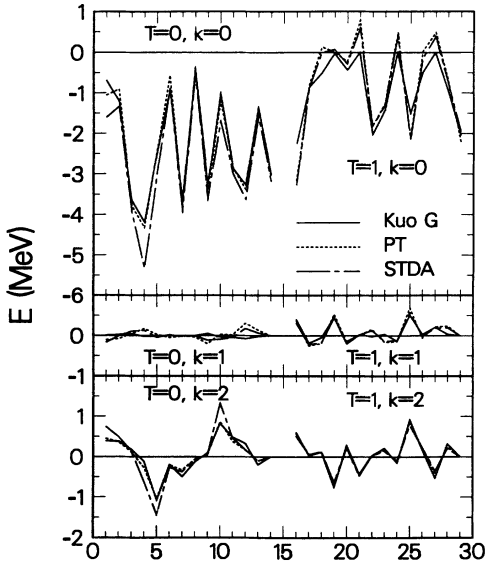

FIG. 3. Spin-tensor decomposition of Hamada-Johnston effective interactions. Shown are the diagonal $T = 0$ (on the left) and $T = 1$ $(1s0d)^2$ matrix elements in jj coupling of the various k components of the interactions defined in Fig. 1. The enumeration of the matrix elements is defined in Table II.

matrix elements (cf. Table II) in the ($1s0d$) shell for the three interactions obtained from the Hamada-Johnston potential. In all cases, the dominant contribution comes from the central term, and thus, the $k = 0$ components roughly reflect the behavior of the spectra in the various approximations. For $T = 1$ the interaction is clearly modified when higher-order terms are added to the bare G interaction. As shown in Fig. 2, the interaction evaluated to second order (PT) is very similar to the interaction evaluated by summing the core-polarization diagrams in the screened Tamm-Dancoff approximation (STDA). The situation is somewhat different for $T = 0$, where the bare G is very similar to STDA but different from PT.

This difference between $T = 1$ and $T = 0$ may be understood in the following way. The STDA is really very similar to the second-order core-polarization diagram [Fig. 1(b)] for both $T = 1$ and $T = 0$. For $T = 1$ this diagram dominates the second-order contributions. Thus, PT and STDA are rather similar for $T = 1$. For $T = 0$ the dominant second-order diagram is the one shown in Fig. 1(c) with four-particle, two-hole intermediate states, whereas the core-polarization diagram of Fig. 1(b) is rather small. Thus G and STDA (which is similar to G plus the second-order core-polarization diagram) are roughly equal, while PT gets the additional contribution from Fig. 1(c).

The vector ($k = 1$) components are seen to be small for both $T = 1$ and $T = 0$. In particular, the $k = 1$ contribution to the bare G matrix is virtually zero for T=0. The only nonzero contribution to the $T = 0$ G matrix elements comes from the interaction in spatially antisymmetric states which is small. On the other hand, the $T = 1$ G matrix is due to the interaction in spatially symmetric states and is much larger. Now, when the interaction is renormalized, both spatially symmetric and antisymmetric components of the bare G interaction will contribute and serve to modify the bare interaction. Although the modifications are small in magnitude, they are certainly large on a relative scale for $T = 0$.

The tensor ($k = 2$) components are small compared to the central components but much larger than the vector components. Some of the $k = 2$ matrix elements are in fact as large as 0.5–1.0 MeV. For $T = 1$ there is little difference in the $k = 2$ components of the bare and renormalized interactions. Some of the $T = 0$ matrix elements are, however, strongly modified in PT. This is due to the diagram of Fig. 1(c), as discussed for $k = 0$ above. It is worth noticing that the $k = 0$ and $k = 2$ contributions from Fig. 1(c) cancel each other for some $T = 0$ matrix elements (e.g., $d^2_{5/2}, J = 1$ and $d^2_{3/2}, J = 1$) and add for others (e.g., $d_{5/2}d_{3/2}, J = 1$ and 2). Comparing the $k = 2$ components for $T = 1$ and $T = 0$, we find that the $T = 0$ matrix elements are only marginally larger in size than the $T = 1$ matrix elements. The tensor force derived from a one-pion-exchange potential would give matrix elements three times as large in the $T = 0$ channel as in the $T = 1$. Thus, not surprisingly, the renormalization procedures involved in calculating the reaction matrix G and the higher-order corrections to G seem to alter the spin-tensor components of the original NN interaction.

B. Meson-exchange potentials

Now we turn to the spin-tensor decomposition of the interactions derived from modern meson-exchange potentials. Figure 4 is analogous to Fig. 3 and shows the corresponding quantities for the three interactions derived from the Bonn-Jülich potential listed in Table I. The results for the corresponding Paris interactions are rather similar, except for the differences associated with the extra repulsion in the $T = 0$ G-matrix elements discussed in Sec. II, and will not be displayed here. It follows from Fig. 4 that the relative strengths of the three k components are rather similar to those shown in Fig. 3. The central component is the dominant one, while the $k = 1$ and $k = 2$ components are fairly small. As for the Hamada-Johnston-based interactions the $k = 1$ component is the smaller one, but it has increased its size relative to $k = 2$ as compared to Hamada-Johnston. Still, the $T = 0$ G-matrix elements have very small $k = 1$ components; these are, however, considerably increased by adding higher-order corrections. The $k = 2$ component is smaller than for the Hamada-Johnston-based interactions, on an absolute scale and particularly on a relative scale, as the

TABLE II. Enumeration of the matrix elements $< j_1 j_2 JT|\nu_k|j_1 j_2 JT >_a$ shown in Figs. 3 and 4.

No.	T	j_1	j_2	J	No.	T	j_1	j_2	J
1	0	$d_{5/2}$	$d_{5/2}$	1	16	1	$d_{5/2}$	$d_{5/2}$	0
2				3	17				2
3				5	18				4
4	0	$d_{5/2}$	$d_{3/2}$	1	19	1	$d_{5/2}$	$d_{3/2}$	1
5				2	20				2
6				3	21				3
7				4	22				4
8	0	$d_{5/2}$	$s_{1/2}$	2	23	1	$d_{5/2}$	$s_{1/2}$	2
9				3	24				3
10	0	$d_{3/2}$	$d_{3/2}$	1	25	1	$d_{3/2}$	$d_{3/2}$	0
11				3	26				2
12	0	$d_{3/2}$	$s_{1/2}$	1	27	1	$d_{3/2}$	$s_{1/2}$	1
13				2	28				2
14	0	$s_{1/2}$	$s_{1/2}$	1	29	1	$s_{1/2}$	$s_{1/2}$	0

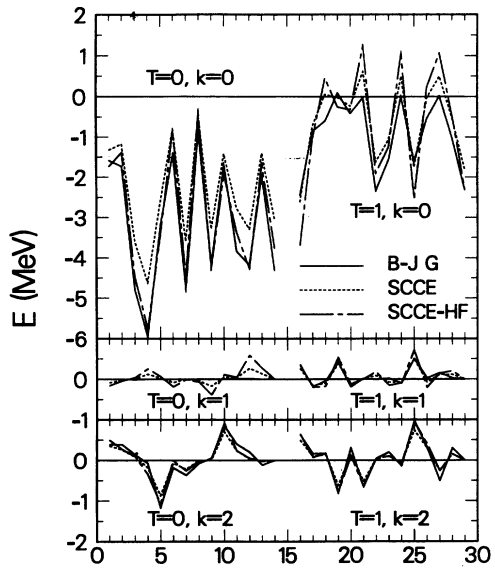

FIG. 4. Spin-tensor decomposition of Bonn-Jülich effective interactions. Shown are the $T = 0$ (on the left) and $T = 1$ diagonal $(1s0d)^2$ matrix elements of the various k components of the interactions defined in Fig. 1. The enumeration of the matrix elements is defined in Table II.

total matrix elements are larger in size. This is presumably due to the strong ρN coupling constant employed in constructing the Bonn-Jülich NN potential and the resulting weaker tensor force, as discussed in Sec. I.

Let us compare the effect of the different renormalizations of the Bonn-Jülich potential on the spin-tensor decomposition. For $T = 1$, the addition of higher-order core-polarization diagrams in the SCCE approximation considerably increases the magnitude of the $k = 0$ matrix elements. The renormalization effect on the $k = 1$ and $k = 2$ matrix elements is rather small. This is indeed very similar to the effect of core-polarization (PT and STDA) on the Hamada-Johnston interaction. For $T = 0$, SCCE is rather similar to G for $k = 0$, but rather different for $k = 1$. This is again similar to what was found for the Hamada-Johnston potential. There is, however, some difference for $k = 2$, as the renormalization seems to have less effect on the Bonn-Jülich $k = 2$ matrix elements than on the Hamada-Johnston ones. To understand this, recall that the renormalization effect on $k = 2$ in the Hamada-Johnston case (Fig. 4) was due to the second-order corrections (PT) and reflected the importance of the diagram of Fig. 1(c). The second-order core-polarization diagram of Fig. 1(b) is similar to STDA and SCCE and has little effect on the $T = 0$, $k = 2$ matrix elements.

Figure 4 also shows the effect of using a Hartree-Fock rather than a harmonic-oscillator single-particle basis for the effective interaction. In the approximation denoted by $(\mathrm{SCCE})_{\mathrm{HF}}$ the input G-matrix elements were evaluated partly with single-particle wave functions resulting from a HF calculation and partly with oscillator single-particle wave functions scaled to imitate the HF effect, as described in Ref. [15]. It is seen that using a HF basis serves to reduce the magnitude of the matrix elements of the SCCE effective interaction, both for $T = 1$ and $T = 0$. For $T = 1$, the $(\mathrm{SCCE})_{\mathrm{HF}}$ is intermediate between G and SCCE, whereas for $T = 0$ it is reduced in magnitude with respect to both G and SCCE, which are similar in magnitude, as pointed out above. This situation is reflected by the A=18 spectra (Fig. 2 for $T = 1$ and the corresponding $T = 0$ spectrum from Ref. [15]) and also shows up in the $k = 0$ components of the interactions. For $k = 1$ and $k = 2$ there is less effect of using a HF basis, except for $T = 0, k = 1$ where renormalization is essential and thus $(\mathrm{SCCE})_{\mathrm{HF}}$ is intermediate between G and SCCE.

We can get a picture of the average difference between SCCE and $(\mathrm{SCCE})_{\mathrm{HF}}$ by considering the energy centroids of the two-particle configurations. In Fig. 5 we show the centroids of the various $(j_1 j_2)$ configurations for the three different values of k. The largest difference among the interactions is found for $k = 0$ and amounts to 150–200 keV for $d^2_{5/2}$, $d_{5/2}d_{3/2}$, and $d^2_{3/2}$ and as much as 550 keV for $s^2_{1/2}$. The latter difference is not surprising in view of the fact that this configuration involves single-particle wave functions with a node.

Thus far we have only shown the spin-tensor decomposition of the matrix elements diagonal in jj coupling. To avoid too many details, we have not shown the off-diagonal matrix elements. The role of the latter can be included, however, by evaluating the spectra for $k = 0$, for $k = 0$ plus $k = 1$, and for all k values included (or by examining the centroids in LS coupling, as we do below). The resulting spectra obtained for G and STDA in the case of the Hamada-Johnston potential are shown in Fig. 6 for $T = 1$ and $T = 0$. For the Bonn-Jülich potential we evaluate the corresponding spectra for G and SCCE; these are shown in Fig. 7 for $T = 1$ and $T = 0$. We see that, for given T, the effect of the various k components

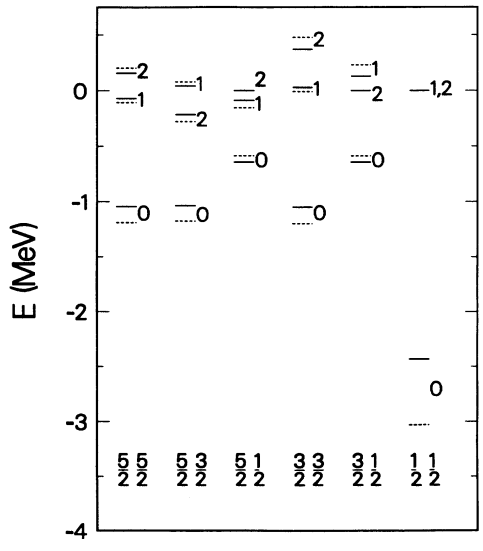

FIG. 5. Isospin averaged energy centroids in jj coupling for the three values of the rank k. The Bonn-Jülich interaction in a harmonic-oscillator (solid lines) and Hartree-Fock (dashed lines) basis was used.

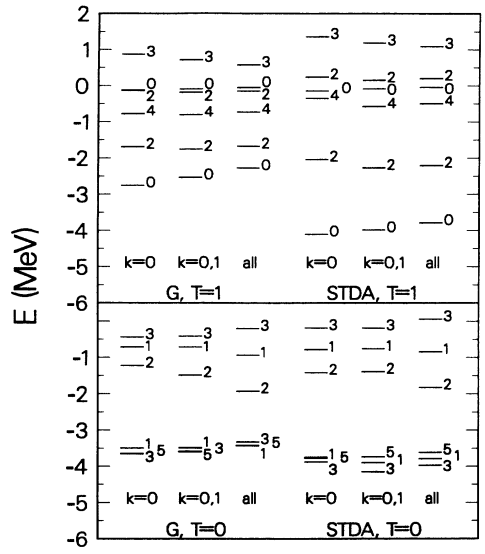

FIG. 6. $A = 18$ spectra obtained with contributions from the various spin-tensor components using the G and STDA (Hamada-Johnston) interactions.

is qualitatively similar for all effective interactions (and NN potentials) considered. The basic structure of the spectrum is given by $k = 0$. The addition of $k = 1$ has, as expected, little effect on the spectrum. The effect of $k = 2$ is small for $T = 1$, but it does serve to compress the spectrum slightly. For $T = 0$, the $k = 2$ component is more important, serving to lower the 2^+ states somewhat. The difference between the various approximations for the effective interactions has been briefly discussed in Sec. II and will not be further discussed here.

In Fig. 8 are shown the $T = 0$ and $T = 1$ energy centroids for the three SU(3) representations that occur for the two-particle system. As previously demonstrated [8]

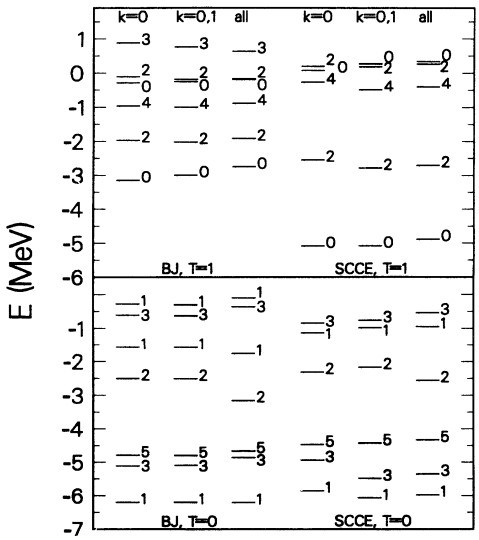

FIG. 7. $A = 18$ spectra obtained with contributions from the various spin-tensor components using the G and SCCE (Bonn-Jülich) interactions.

there can be large differences in the SU(3) centroids even if the differences among the jj centroids are small. The dominant contribution to the energies of low-lying levels arises from the contributions from the (4 0) representation. As seen in Fig. 8, in going from an oscillator basis to a Hartree-Fock basis results in approximately 1 MeV less binding for the $A = 18$ system; this implies there would be a 4 to 6 MeV difference in ^{20}Ne. Similarly, the Bonn-Jülich interaction provides approximately 1 MeV more binding than does the Paris interaction. The old Kuo-Brown interaction [11] does a reasonable job in describing both spectra and binding [19]. The indication from Fig. 8 is that the Bonn-Jülich in an oscillator basis will overbind ($1s0d$) nuclei while the Bonn-Jülich and the Paris interaction in a Hartree-Fock basis will underbind. The latter was already known from the work of Shurpin [8] (by about 4 MeV in the A=22 system) and in which it was also shown that folded diagrams exacerbate the problem.

The T=1 interaction is less sensitive to a change in the single-particle wave function: moving from an oscillator basis to a Hartree-Fock basis results in a change in the centroid of **[2]** of 0.4 MeV for the T=1 and 1 MeV for the T=0 Bonn-Jülich interaction. The results are smaller for the Paris interaction. Most of this change occurs for the (4 0) representation. The (0 2) centroids are less affected. This presumably is a result of such effects being maximized for relative $0s$ states; only the (4 0) representation contains relative $0s$ states. Similarly, moving from the oscillator basis to a Hartree-Fock basis moves the

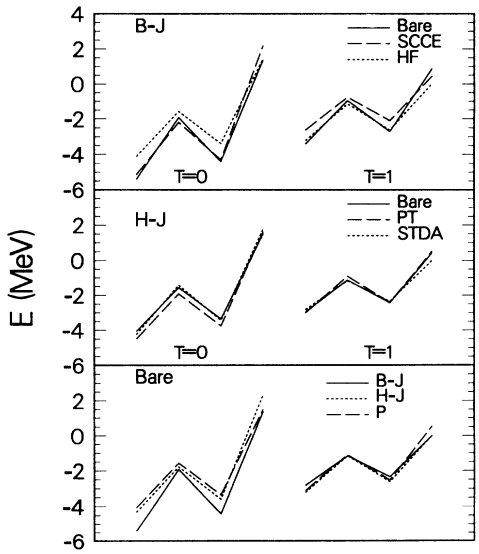

FIG. 8. Two-particle SU(3) and SU(4) energy centroids for the interactions discussed in this paper. For each interaction, the left curve is for T=0, the right for T=1. In each curve the four points are, from left to right, (4 0), (0 2), **[2]**, and (2 1). The centroid for **[11]** coincides with that for the SU(3) representation (2 1). The top two subplots illustrate the effects of including core renormalization corrections; the lowest subplot shows centroids for the bare interaction of three potentials. For each interaction and isospin the (4 0) lies lowest and the (2 1) highest with the (0 2) in the middle.

[11] centroid down in energy by approximately 1 MeV. Thus, SU(4) may be expected to be less valid in the self-consistent basis.

Other than the pioneering work of Pluhař [20], no SU(3) tensor decomposition of ($1s0d$) shell interactions has been reported although such a decomposition is in regular use in the SU(3) shell model code of Millener [21]. Pluhař only decomposed the Kuo interaction, but did not make any comparison among different interactions. In Fig. 9 are shown values of the dominant SU(3) tensors having rank zero for six interactions discussed in this paper. Also shown are the results for the Chung-Wildenthal interaction [22] obtained by fitting 63 two-body matrix elements to spectra of $1s$-$0d$ nuclei. The largest tensor by far is the one with quantum numbers $[(40) \times (04)]^{(00)}$. The next largest is $[(02) \times (20)]^{(00)}$ while operators with the same two-body $(\lambda\mu)$, but coupled to (2 2), are somewhat smaller. Matrix elements of other SU(3) tensors tend to be even smaller. The above matrix elements are of tensors that are SU(4) scalars and thus conserve SU(4) symmetry. Other tensors can violate SU(4) but their matrix elements are a factor five to ten smaller than those that conserve SU(4). Of course the importance of each of the terms depends not only on the magnitude of the tensor, but also on the magnitude of the recoupling coefficient that multiplies the tensor. These factors will vary with particle number and SU(3) and SU(4) representation of the A-particle basis state.

Extremely large differences among the interactions show up in the matrix elements of $[(40) \times (04)]^{(00)}$; these differences may be as large as 5 MeV when changing from an oscillator basis to a Hartree-Fock basis. Interestingly,

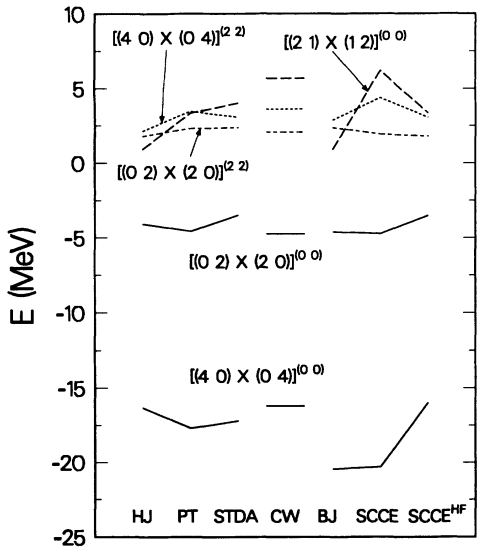

FIG. 9. The values of two-body matrix elements of selected SU(3) tensors for each of the several interactions discussed in this paper. The SU(4) representation for each tensor is **[2222]** or an SU(4) scalar. The matrix elements for the tensors having rank **[422]** are factors of five to ten smaller and are not shown. Results for the Chung-Wildenthal [22] interaction are denoted by CW.

the matrix elements of other operators do not show large variations; the largest are for the tensors $[(02) \times (20)]^{(00)}$ and $[(40) \times (04)]^{(22)}$. The variation in the matrix elements for other zero rank tensors is on order of tens of keV or less. This suggests that when fits of two-body interactions to experiment are performed, it might be most efficient to fix most of the two-body matrix elements and only vary these few linear combinations of matrix elements, particularly as contributions from [(40)] dominate the wave functions of low-lying states in the $1s$-$0d$ shell.

V. SUMMARY AND CONCLUSIONS

We have analyzed several realistic shell model effective interactions, which have proven successful in reproducing nuclear properties, for their spin-tensor components. The effective forces examined were obtained from the phenomenological Hamada-Johnston potential as well as the meson-exchange Bonn-Jülich and Paris potentials and were calculated to various approximations. For the Hamada-Johnston potential the effective interaction was calculated to first- (G) and second-order (PT) in the reaction matrix G. In addition we considered an interaction obtained by summing the core-polarization diagrams to all orders using particle-wave vertices screened to second order (STDA). For the Bonn-Jülich and Paris potentials we considered the bare G and a renormalized interaction including essentially all long-range correlations self-consistently to arbitrary order (SCCE). The latter interaction was also evaluated using a Hartree-Fock rather than a harmonic-oscillator single-particle basis, the resulting interaction being denoted by $(\mathrm{SCCE})_{\mathrm{HF}}$.

For all forces examined, the dominant contribution comes from the central part. Thus, the central part seems to be sufficient to produce the basic structure of the spectra for *two* nucleons outside closed shells. The effect of renormalization of the bare G matrix may be substantial. For $T = 1$, the core polarization, whether to second or higher order, may produce significant effects. For $T = 0$, the diagram of Fig. 1(c) with four-particle, two-hole intermediate states seems to be more important than the core-polarization diagram of Fig. 1(b). When HF single-particle wave functions are used instead of the usual harmonic-oscillator ones, the k=0 components are considerably reduced in size. For T=1 they are intermediate between G and SCCE whereas for T=0 they are considerably smaller in size than G (which is similar to SCCE). Centroids in j-j and SU(3) coupling were obtained with and without noncentral contributions; considerable sensitivity was observed in the SU(3) basis.

The vector component is small for the bare G-matrix interaction, especially for $T = 0$, but is considerably modified by renormalization. Anyway, it has only little effect on the energy spectra for two valence nucleons. The tensor component is somewhat larger than the vector component and is relatively larger for the Hamada-Johnston potential than for the Bonn-Jülich and Paris potentials. This is not surprising in view of the stronger tensor-force component in the original Hamada-Johnston NN potential. The effect of the tensor component on the two-valence-nucleon spectra is fairly small, particu-

larly for $T = 1$. It does, however, serve to compress the spectrum slightly. The effect on the $T = 0$ spectrum is somewhat larger, the main effect being to lower the 2^+ levels, especially the second one. Although the effect of the vector and tensor components on the spectra of two valence nucleons is small, it is likely to increase with the number of valence nucleons. Thus, it would be of considerable interest to study their effect on many-valence-nucleon spectra, and such calculations are under way.

As pointed out above, it is not straightforward to establish the correspondence between the different k components in the original NN interactions and the renormalized effective interaction. In fact, a strong tensor force in the NN interactions will produce a strong central contribution to second order in the G matrix [23]. Still, it seems that the strength of the tensor component in the NN interaction is reflected in the renormalized interactions. Thus, for the convergence of the effective interaction it seems desirable to start from an NN interaction with a weak tensor force, which favors a strong ρN coupling constant.

We wish to thank Anna Hayes for numerous discussions and comments.

[1] T. Hamada and I. D. Johnston, Nucl. Phys. **34**, 382 (1962) .
[2] R. V. Reid, Ann. Phys. (N.Y.) **50**, 411 (1968).
[3] M. Lacombe *et al.*, Phys. Rev. C **21**, 861 (1980).
[4] M. R. Anastasio, A. Faessler, H. Müther, K. Holinde, and R. Machleidt, Phys. Rev. C **18**, 2416 (1978).
[5] M. R. Anastasio and G.E. Brown, Nucl. Phys. **A285**, 516 (1977).
[6] D. Strottman, Nucl. Phys. **A188**, 488 (1972).
[7] M. W. Kirson, Phys. Lett. **47B**, 110 (1973).
[8] J. Shurpin, T. T. S. Kuo, and D. Strottman, Nucl. Phys. **A408**, 310 (1983).
[9] B. A. Brown *et al.*, J. Phys. G **11**, 1191 (1985).
[10] B. A. Brown *et al.*, Ann. Phys. (N.Y.) **182**, 191 (1988).
[11] T. T. S. Kuo and G. E. Brown, Nucl. Phys. **85**, 40 (1966); T. T. S. Kuo, *ibid.* **A103**, 1 (1967).
[12] T. T. S. Kuo and E. Osnes, Nucl. Phys. **A226**, 204 (1974).
[13] J. Shurpin, Ph. D. thesis, State University of New York at Stony Brook, 1980 (unpublished).
[14] M. Sommermann *et al.*, Phys. Rev. **23**, 1765 (1981).
[15] S. Chakavarti *et al.*, Phys. Lett. **109B**, 141 (1982).
[16] P. J. Ellis and T. Engeland, Nucl. Phys. **A144**, 161 (1970).
[17] M. Conze, H. Feldmeier, and P. Manakos, Phys. Lett. **43B**, 101 (1973).
[18] J. P. Draayer and Y. Akiyama, J. Math. Phys. **14**, 1904 (1973).
[19] E. C. Halbert *et al.*, in *Advances in Nuclear Physics*, edited by M. Baranger and E. Vogt (Plenum, New York, 1970), Vol. 4.
[20] Z. Pluhař, Nucl. Phys. **A167**, 33 (1973).
[21] D. J. Millener, private communication.
[22] W. Chung, Ph.D. thesis, Michigan State University, 1976 (unpublished).
[23] G.E. Brown, *Unified Theory of Nuclear Models and Forces* (North-Holland, Amsterdam, 1971).